HIGH PRECISION AL-MG CHRONOLOGY OF CHONDRULES IN UNEQUILIBRATED ORDINARY CHONDRITES.

G. Siron[1], N. T. Kita[1], K. Fukuda[1], and M. Kimura[2]. [1]WiscSIMS, Department of Geoscience, University of Wisconsin-Madison, Madison, WI 53706, USA (siron@wisc.edu, noriko@geology.wisc.edu), [2]National Institute of Polar Research, Meteorite Research Center, Tachikawa, Tokyo 190-8518, Japan.

Introduction: The ^{26}Al-^{26}Mg chronology of chondrules can provide key constraints on their formation mechanism, under the assumption of a homogeneous distribution of ^{26}Al (half-life: 0.705 million years; Ma) in the early Solar System [1]. Unequilibrated ordinary chondrites (UOCs) contain chondrules with high Na concentrations, which likely formed in high-density protoplanetary disk and had accreted immediately (<0.1 Ma) to the parent asteroidal bodies [2-3]. However, both Al-Mg and Pb-Pb ages of UOC chondrules show a long period from 1.5-3.0 Ma and 0-4 Ma after the formation of Ca, Al-rich inclusions (CAIs), respectively [4-6]. [3] argued that the parent body processes might have disturbed these chronometers.

Recently [7] reported high precision Al-Mg analyses of 14 anorthite-bearing chondrules in low subtype (3.01 -3.05) UOCs in order to minimize the effect of parent body disturbance. The results show a narrow range of $(^{26}\mathrm{Al}/^{27}\mathrm{Al})_0$ from $(6.3\pm0.7)\times10^{-6}$ to $(8.9\pm0.3)\times10^{-6}$, corresponding to ages from 1.80±0.04 Ma to 2.16±0.12 Ma after CAIs. While these data indicate a short duration for formation of UOC chondrules, as suggested by [2-3], anorthite-bearing chondrules are an uncommon subset of chondrules depleted in Na. Therefore, these results may not represent the total range of OC chondrule formation ages. Here we further report high precision Al-Mg ages of 17 chondrules in UOCs that contain a wide range of plagioclase compositions and glassy mesostasis with high Al/Mg ratios, most of which are enriched in Na.

Samples and Methods: Chondrules were selected from Queen Alexandra Range (QUE) 97008 (L3.05), Northwest Africa (NWA) 7731 (L3.00), NWA 8276 (L3.00), Meteorite Hills (MET) 00452 (L/LL3.05), NWA 8649 (LL3.05), and Semarkona (LL3.01). They include 11 and 6 chondrules from L and LL chondrites, respectively. They were first examined by SEM-EDS. Compositions of mineral and glass were determined by a EMPA Cameca SX51 and FE-EPMA SX Five. For accurate aiming of small (<10 μm) plagioclase and glass using SIMS, we applied FIB marks using a FE-SEM Zeiss Auriga with FIB capability according to the method described in [8].

Al-Mg isotope analyses were conducted using the Cameca IMS 1280 SIMS equipped with RF plasma ion source. Mg isotope analyses of plagioclase and glass were obtained using a 45 pA O_2^- primary beam (4 μm in size) and three electron multipliers on multi-collector trolleys for simultaneous detection (MCEM), similar to those described in [8]. Several analyses of plagioclase and glass with higher MgO (0.3-1%) were conducted by using 160 pA primary beam (~6 μm) and Faraday Cup (FC) for $^{24}\mathrm{Mg}^+$ and EM for $^{25}\mathrm{Mg}^+$ and $^{26}\mathrm{Mg}^+$ (FCEM) according to the condition in [7]. The $^{27}\mathrm{Al}^+$ was always detected by using MCFC. Typical analytical uncertainties of $\delta^{26}\mathrm{Mg}^*$ were 1.6-2‰ for labradorite (An_{60}) standard with MgO ~0.1% using MCEM condition and ~0.4‰ for anorthite glass standard with 1% MgO using FCEM condition. Olivine and pyroxene were analyzed using 1 nA primary beam (~8 μm) and MCFC condition with precision of 0.05‰ for $\delta^{26}\mathrm{Mg}^*$ [7].

Results: Fourteen chondrules includes plagioclase with a wide range of An contents from An_1 to An_{87}, and three other chondrules contain glassy mesostasis with high $\mathrm{Na_2O}$ contents and low MgO (0.1-0.4%). They show porphyritic textures (1 PO, 7 POP, and 9 PP) with a wide range of Mg# (=[Mg]/[Mg+Fe] molar%) in olivine and pyroxene from 77 to 98. Plagioclase An contents generally increase with increasing Mg# of chondrules. Three plagioclase-bearing chondrules contain small area of glassy mesostasis, in which both plagioclase and glass were analyzed for Al-Mg data.

Plagioclase and glass in all 17 chondrules show high $^{27}\mathrm{Al}/^{24}\mathrm{Mg}$ (>100) and resolvable excess $\delta^{26}\mathrm{Mg}^*$ that correlate with $^{27}\mathrm{Al}/^{24}\mathrm{Mg}$ ratios. Large excesses of $\delta^{26}\mathrm{Mg}^*$ (50-140‰) was found among chondrules with albite-rich plagioclase. Exceptions are glassy mesostasis in two of plagioclase-bearing chondrules that did not show resolvable $\delta^{26}\mathrm{Mg}^*$ (Fig. 1).

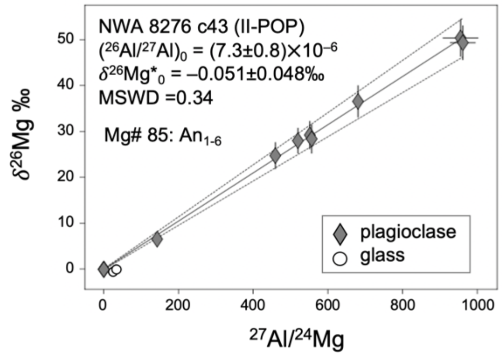

Fig. 1. An example of Al-Mg isochron of UOC chondrules in this study. Error bars are propagated 2σ uncertainties of each analysis. Glass analyses without ^{26}Mg excess are not included in the regression. Error envelope are 95% confidence interval on the fit.

The regression of Al-Mg data from individual chondrules show inferred (^{26}Al/^{27}Al)$_0$ ratios from (6.5±0.6) ×10^{-6} to (9.5±1.0)×10^{-6}, which are in the same range as anorthite-bearing chondrules by [7] (Fig. 2). MSWD of regression lines are in a range from 0.34 to 1.8. They correspond to ages from 1.74±0.12 Ma to 2.13 ±0.09 Ma relative to CAIs with (^{26}Al/^{27}Al)$_0$ = 5.25×10^{-5} [9]. These data are in good agreement with most of the UOC chondrule data from the literature, within their uncertainties [e.g., 1, 4-5 and references therein].

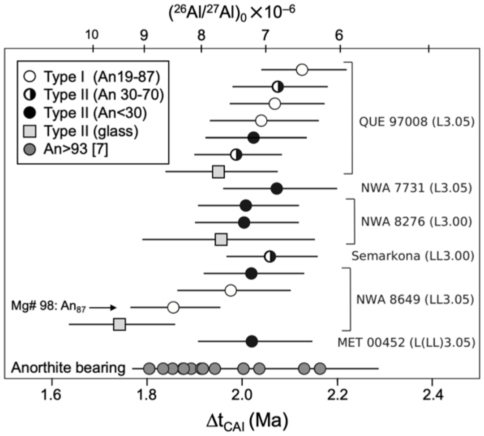

Fig. 2. Summary of inferred (^{26}Al/^{27}Al)$_0$ among UOC chondrules from this study and [7].

Discussions: New results from 17 chondrules in this study and [7] show a restricted range of relative ages within 0.4 Ma (1.8-2.2 Ma after CAIs). Except for two chondrules with older ages ~1.8 Ma (one glass-bearing and one type I PP), all chondrules show indistinguishable ages with a mean of 2.03±0.10 Ma (2SD). This is consistent with the peak of ages determined by [4]. Interestingly, six type II chondrules with albite-rich plagioclase (An<30) show a small range of nominal ages from 2.00 to 2.07 Ma after CAIs, which may support a short duration of chondrule formation (<0.1 Ma) in high density disk as proposed by [2-3].

Including data from [7], we did not find any chondrules with relative ages younger than 2.2 Ma, in contrast to data obtained by [4-5] (Fig. 3). Younger chondrule ages by [5] might represent multiple heating events [10]. However, the two dataset differ significantly in the SIMS analytical approaches. [4-5] used large and intense primary beam (~30 µm) for the analyses of MgO-rich glassy mesostasis with a high precision MCFC setting, though analyses tend to overlap with adjacent mafic minerals. As indicated from glass analyses in this study without resolvable excess δ^{26}Mg*, glassy mesostasis are more susceptible to disturbance in Al-Mg system by parent body metamorphism. Overlapping analyses could have include altered phases in grain boundaries where radiogenic ^{26}Mg could have been lost. Thus, we consider that UOC chondrule formation likely ended by 2.2 Ma, which is consistent with the time of accretion of ordinary chondrite parent bodies estimated from thermal models [e.g., 11].

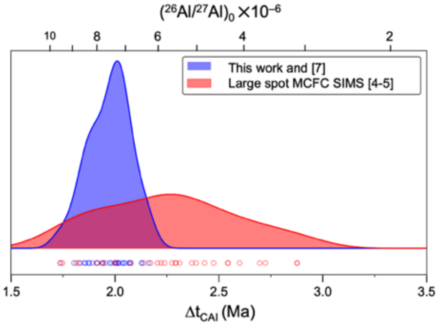

Fig. 3. Kernel density function for (^{26}Al/^{27}Al)$_0$ among UOC chondrules from this study and [7] compared to MCFC data for glass-bearing chondrules by [4-5].

As indicated by [5], there are no chondrules with (^{26}Al/^{27}Al)$_0$ higher than 1×10^{-5} from internal isochron methods. This may indicate that no chondrules formed in the ordinary chondrite forming regions until 1.8 Ma. This timing could be related to growth of proto-Jupiter, protoplanets, and large planetesimals that would be required to trigger chondrule forming transient heating mechanisms [e.g., 12-13]. Chondrules in carbonaceous chondrites typically show lower (^{26}Al/^{27}Al)$_0$ ≤6×10^{-6} [e.g., 14], which may indicate growth of planetary bodies would be slower in the outer protoplanetary disk compared to inner regions .

Summary: New high precision Al-Mg dating of UOC chondrules indicate a short duration for their formation from 1.8 to 2.2 Ma after CAIs. The timing would be constrained by the growth of planetary bodies in the ordinary chondrite chondrule forming regions and the accretion of their parent bodies.

References: [1] Kita N. T. and Ushikubo T. (2012) *MaPS, 47,* 1108-1119. [2] Alexander C. M. O'D. et al. (2008), *Science, 320,* 1617–1619. [3] Alexander C. M. O'D and Ebel D. S. (2012) *MaPS, 47,* 1157-1175. [4] Villeneuve J. et al. (2009) *Science, 325,* 985-988. [5] Pape J. et al. (2019) *GCA, 244,* 416-436. [6] Bollard J. et al. (2017) *Sci. Adv. 3,* e1700407. [7] Siron G. et al. (2021) *GCA, 293,* 103-126. [8] Hertwig A. T. et al. (2019) *GCA, 253,* 111-126. [9] Larsen K. K. et al. (2011) *Ap. J., 735,* L37. [10] Pape J. et al. (2021) *GCA 292,* 499-517. [11] Blackburn T. et al. (2017) *GCA, 200,* 201-217. [12] Desch S. J. et al. (2012) *MaPS 47,* 1139-1156. [13] Johnson B. C. et al. (2015) *Nature, 517*, 339-341. [14] Nagashima K. et al. (2018) *In Chondrules: Records of Protoplanetary Disk Processes,* pp. 247–275.